Geophysical Research Letters

RESEARCH LETTER
10.1029/2018GL081587

Focal Mechanisms for Subcrustal Earthquakes Beneath the Gibraltar Arc

Nerea Santos-Bueno[1,2], Carlos Fernández-García[1,3], Daniel Stich[1,4], Flor de Lis Mancilla[1,4], Rosa Martín[1], Antonio Molina-Aguilera[1,4], and Jose Morales[1,4]

[1]Instituto Andaluz de Geofísica, Universidad de Granada, Granada, Spain, [2]Now at Departamento de Ciencias de la Tierra, Universidad de Zaragoza, Zaragoza, Spain, [3]Now at Université Rennes, CNRS, Géosciences Rennes-UMR, Rennes, France, [4]Departamento de Física Teórica y del Cosmos, Universidad de Granada, Granada, Spain

Key Points:
- Receiver function images and earthquake locations suggest a buried corridor of autochthonous oceanic lithosphere between Iberia and Africa
- Subcrustal focal mechanisms beneath the Gibraltar Arc do not support active subduction
- Most mechanisms agree with shear from relative plate motion or drag from absolute plate motion

Supporting Information:
- Supporting Information S1

Correspondence to:
D. Stich,
stich@ugr.es

Citation:
Santos-Bueno, N., Fernández-García, C., Stich, D., Mancilla, F. d. L., Martín, R., Molina-Aguilera, A., & Morales, J. (2019). Focal mechanisms for subcrustal earthquakes beneath the Gibraltar Arc. *Geophysical Research Letters*, *46*, 2534–2543. https://doi.org/10.1029/2018GL081587

Received 30 JAN 2019
Accepted 26 FEB 2019
Accepted article online 4 MAR 2019
Published online 13 MAR 2019

Abstract Intermediate deep earthquakes are usually associated with active subduction, and show mostly dip-slip faulting mechanisms aligned with the downgoing oceanic lithosphere. Forty-two new focal mechanisms from 50- to 100-km depth beneath the Gibraltar Arc and Alboran Sea show different characteristics. The most abundant solutions are strike-slip mechanisms, in agreement with relative plate motion between Nubia and Eurasia. Additional reverse faulting mechanisms indicate compression in direction of absolute plate motion, reproducing the basal drag of the mantle on the hanging lithosphere. In turn, no signature of ongoing subduction was found. Migrated sections of *P* wave receiver functions suggest that a significant part of intermediate deep seismicity is produced within the stalled remnants of Jurassic age, oceanic lithosphere that once formed the connection between the Alpine Tethys and the central Atlantic and later has been buried beneath the Gibraltar Arc.

Plain Language Summary Earthquakes below 50-km depth are usually associated with active subduction, and the direction of faulting is aligned with the orientation of the subduction zone. Faulting in 42 earthquakes beneath the Gibraltar Arc and Alboran Sea shows different characteristics. The most abundant solutions show horizontal slip, in agreement with relative plate motion between Africa and Europe. Further solutions are associated with shortening and suggest compression from the basal drag of the Earth's mantle on the moving plates. In turn, no signature of active subduction was found. Images of the Earth's interior from teleseismic waves suggest a relation between the earthquakes and a stalled remnant of ~150-Ma-old oceanic material that once formed the connection between two oceans and later has been buried beneath the Gibraltar Arc.

1. Introduction

The Gibraltar Arc is a tightly curved Orogene that connects the Alpine mountain belts in Southern Spain and Northern Morocco across the Strait of Gibraltar. It separates the Alboran Sea, the western termination of the Mediterranean, from the Gulf of Cadiz and Atlantic Ocean to the west. The region is subject to widespread, moderate seismicity, responding to the oblique, WNW-ESE convergence between Eurasia and Nubia at rate of ~5 mm/year, as well as extensional processes in the Alboran region since the Miocene (e.g., Koulali et al., 2011; Stich et al., 2006). Seismicity in the area includes shallow and intermediate deep earthquakes and isolated, deep events in the mantle transition zone (~600 km; e.g., Buforn et al., 2011). Intermediate deep seismicity concentrates between 50- and 100-km depth, in a 150-km-long band that stretches from southern Spain into the Alboran Sea (Figure 1). Within this band, we can distinguish more intense activity within three clusters located beneath the center of the Western Alboran Sea, in front of the Spanish coast, and onshore, respectively. Intermediate deep seismicity terminates abruptly toward east, while scattered subcrustal events do occur in a ~200-km-wide band toward west.

Models to explain Alboran extension (Comas et al., 1992) and the presence of intermediate deep earthquakes are still discussed controversially. Proposed mechanisms include delamination of subcontinental lithosphere (Calvert et al., 2000; Mancilla et al., 2013; Seber et al., 1996), extensional collapse (Platt & Vissers, 1989), rollback of an eastward dipping lithospheric slab (Faccenna et al., 2004; Lonergan & White, 1997; Spakman & Wortel, 2004), or ongoing subduction (Gutscher et al., 2002, 2012). All these hypotheses honor the existence of a high-velocity anomaly in the upper mantle beneath the Alboran

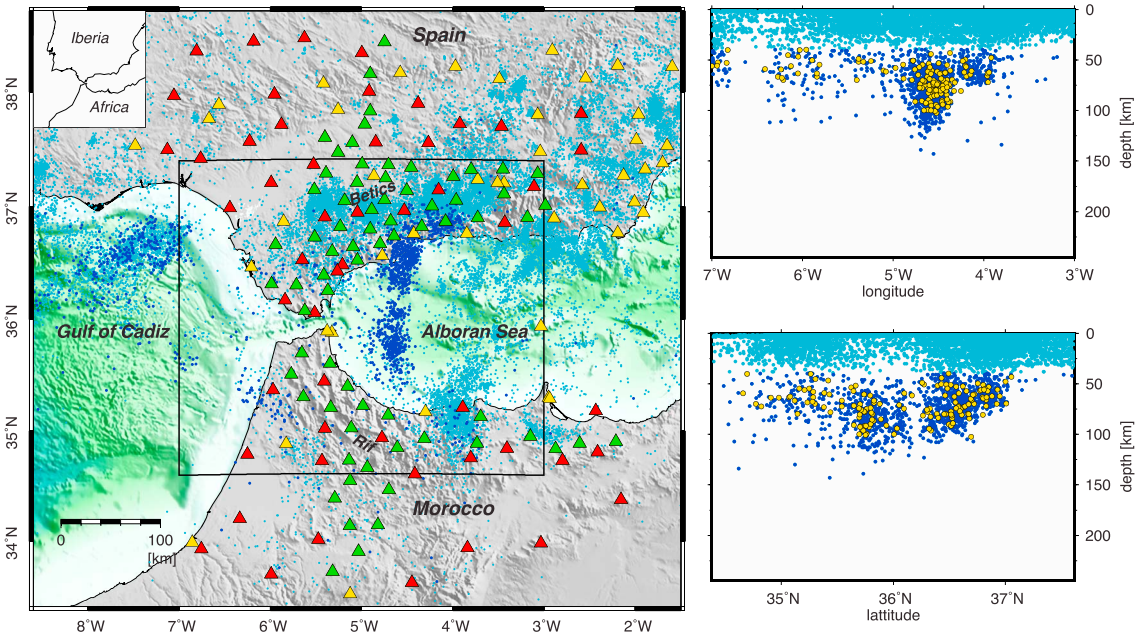

Figure 1. Map showing seismicity of the Gibraltar Arc and surrounding area (light blue for earthquakes at normal depths less than 40 km, dark blue for events larger equal 40 km; deeper events, hypocenters according to Instituto Geográfico Nacional catalogue 2015–2017; only locations with depth are taken; those without assigned depth are dropped). Grid: Gebco 2014. Permanent stations in yellow, stations from the TopoIberia deployment used in red, and stations used from the Picasso deployment in green. The black box outlines the study area. Right side: projection of hypocenters within the study area onto E-W (top right) and S-N (bottom right) vertical sections. Light and dark blue like map; yellow for hypocenters relocated in this study.

region. Recent tomographic images show the steep-dipping, narrow and curved Alboran slab with unprecedented detail (Bezada et al., 2013; Bonnin et al., 2014; Fichtner & Villaseñor, 2015; Palomeras et al., 2014, 2017), strengthening interpretations in terms of subduction-related processes. Still, recent tomographic models disagree on the shallow structure (50–100 km) and lack resolution to clarify the geometric relationship between the slab and intermediate deep earthquakes. In particular, there is no consensus on whether the slab is detached (Palomeras et al., 2014; Piromallo & Morelli, 2003) or connected to the surface (Bezada et al., 2013; Spakman & Wortel, 2004), and whether the shallow part represents lithosphere of oceanic (Gutscher et al., 2002) or continental origin (Palomeras et al., 2014; Thurner et al., 2014). In this study, we aim at a better understanding of the structural context and ongoing deformation in the intermediate deep seismic zone.

Most intermediate earthquakes worldwide occur along recognized slabs and show predominately dip-slip focal mechanisms with principal strain axes aligned close to the strike, dip, and normal vectors of the slab (Chen et al., 2004; Christova & Scholz, 2003; Myhill & Warren, 2012). Beneath the Gibraltar Arc and Alboran Sea, few mechanisms are available for intermediate deep earthquakes, and the solutions appear heterogeneous. Eight seismic moment tensor mechanisms for depths greater 40 km (Buforn & Coca, 2002; Martín et al., 2015) show a tendency toward one subvertical and one subhorizontal nodal plane, however with variable azimuthal orientations. Focal mechanisms from *P* wave first motions (Buforn et al., 2004; Medina, 2008) are available mainly from below the Spanish coast. They show a heterogeneous pattern of normal, reverse, and strike-slip faulting with variable orientation, but in part could fit with deformation in a southeast dipping slab (Ruiz-Constán et al., 2011). The conditions for focal mechanism retrieval improved considerably with the deployment of two dense temporary networks of seismic broadband stations around the Alboran Sea, during the IberArray and Picasso projects from 2007 to 2012 (Gallart et al., 2012; Levander et al., 2009). We use data from temporary and permanent stations during this period to obtain new source mechanisms for intermediate depth earthquakes, deduce the characteristics of deformation in the uppermost mantle, and compare earthquake locations to images of Earth structure from migration of *P* wave receiver functions.

2. Focal Mechanism Inversion

Intermediate deep earthquakes in the study area show mostly low magnitudes, and we recur to first motion polarities to reconstruct the source radiation patterns from local and near-regional recordings. Subcrustal earthquakes are suitable targets for this technique: *P* wave arrivals tend to be clearer and more impulsive compared to shallow earthquakes, and often a wider range of takeoff angles contributes to the coverage of the focal sphere. In addition, takeoff angles are more stable than for shallow events, where modeled angles may be very sensitive to minor changes of source depth or crustal structure. For focal mechanism retrieval we investigate all earthquakes with magnitude m_b larger or equal 2.5 in the IGN catalogue (Instituto Geográfico Nacional, www.ign.es), between longitude 7°W and 3°W and latitude 34.6°N to 37.4°N (Figure 1). From November 2007 to October 2012, 408 events fulfill these criteria, 198 of them with catalogue locations below 40-km depth. We analyze data from a total of 168 stations (Figure 1), although the Picasso and IberArray networks operated with only minor overlap in time, and the amount of available stations for individual events is less.

Prior to focal mechanism inversion, we relocate the earthquakes using Hypocenter (Lienert & Havskov, 1995). *P* and *S* arrivals are picked manually on available waveforms. We tested two different layered Earth models, the one used for earthquake location at IGN (Rueda, 1995) and the one used at IAG for moment tensor inversion (Stich et al., 2003). Both models lead to similar residuals (average root-mean-square of 0.89 s and 0.90 s, respectively) and locations. Average residuals at individual stations show a smooth pattern resembling the crustal thickness map (Mancilla & Diaz, 2015), suggesting that residuals are largely driven by regional-scale wave speed anomalies. We keep for further analysis 145 events located from at least 10 arrival picks, root-mean-square error less than 2 s, and hypocenter depths greater 40 km. Differences between relocated hypocenters and the IGN catalogue are around 10 km. The most systematic change is an eastward shift of the intermediate depth seismicity cluster in the central Alboran Sea (Figure 1). The depth distribution of intermediate deep earthquakes becomes clearer from the relocated dataset. Maximum depths are ~100 km in the N-S trending lineament beneath the Alboran Sea, and clearly less (~70 km) beneath the South Spanish coast and Gibraltar Arc. We did not find intermediate deep seismicity east of 4.3°W at the Moroccan coast, and east of 3.6°W at the Spanish coast.

We carefully pick polarities of impulsive *P* wave arrivals on vertical component seismograms. A grid search scheme (FocMec; Snoke et al., 1984) is used to test the full range of nodal plane orientations of double couple mechanisms with 10° increments. Takeoff angles were computed in the IGN velocity model (Rueda, 1995). Sensor polarities were verified with recordings from teleseismic earthquakes. We exclude all solutions with two or more polarity error, azimuthal gap larger than 120°, or any fundamental ambiguity among the solution set provided by the grid search, keeping a total of 42 credible solutions (Figure 2 and Table S1 in the supporting information). A median of 23 polarity readings has been used, and mechanisms have a typical resolution of ~20° (Kagan, 2007; Table S1). Magnitudes range from m_b 2.5 to m_b 5.4 (IGN catalogue). Only for one inverted mechanism (22 April 2010; m_b 5.4), a moment tensor estimate is available for comparison (Martín et al., 2015), showing a fair agreement of source depth (60 vs. 70 km in this study) and mechanism (Figure 2), however indicating moment magnitude Mw 3.9, which suggests that a significant overestimation of routine catalogue magnitudes may occur for intermediate deep events in the study area.

3. Intermediate Deep Deformation

The obtained mechanisms achieve a broad coverage of the intermediate depth seismicity zone, including the principle seismicity clusters, as well as the diffuse seismicity beneath the Gibraltar Arc (Figure 3). Mechanisms are heterogeneous with regard to faulting style and principle axes orientations. The inventory even includes solutions with nearly opposite kinematics, sometimes at nearby locations, and cannot be plausibly associated with a uniform stress field. In particular, the population of mechanisms is fundamentally different from the simple pattern of oriented, dip-slip focal mechanisms commonly observed in subducting slabs. To unravel the complex characteristics of subcrustal faulting, we classify the solutions into reverse, strike slip and normal faulting style, according to the attributes of the steepest dipping principal strain axes (*T*, *N*, or *P* axes; Figure 3).

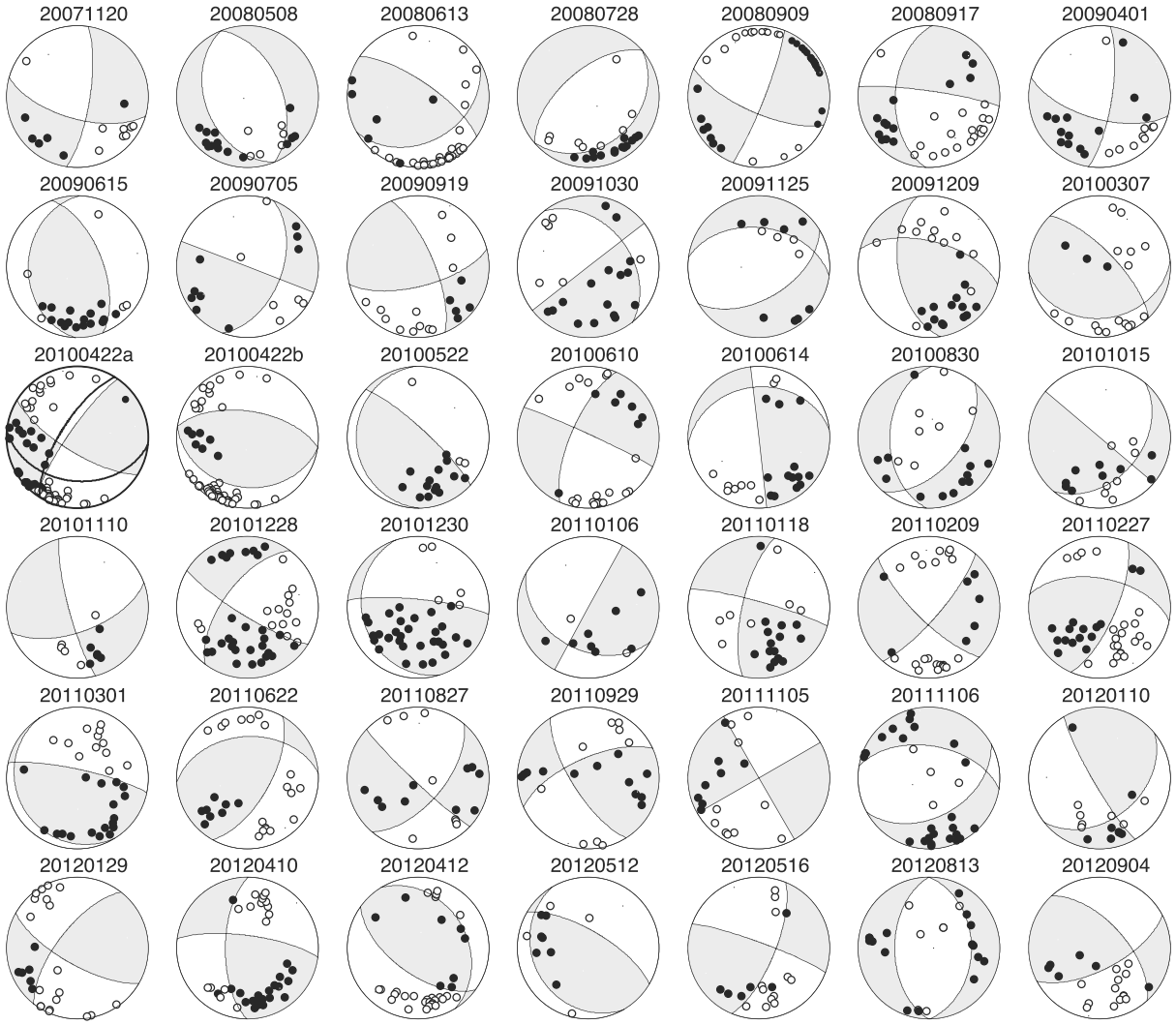

Figure 2. Obtained focal mechanisms in order of earthquake occurrence. Observations of vertical *P* wave first motions in upward (black dots) and downward (open circles) directions are shown in lower hemisphere, equal-area projection. Each mechanism is labeled with the date of the earthquake (year, month, day) for comparison with Figure 3 and table S1. On mechanism 20100422a, an available moment tensor mechanism is superposed for comparison.

Reverse faulting is found for 12 solutions, representing close to 30% of the inverted mechanisms. Reverse faulting solutions are more abundant in the southern sector, beneath the central Alboran Sea and Northern Morocco, and less frequent near the Spanish coast. All but one of the solutions show similar orientations of *P* axes in NE-SW direction (Figures 3, S2, and S3). This orientation has no obvious relationship with the directions of the intermediate deep hypocenter distribution, or the deep Alboran slab inferred from tomographic models (e.g., Bonnin et al., 2014; Fichtner & Villaseñor, 2015), and thus appears unrelated to active subduction. The direction of compression is similar to the peculiar SW motion of the Rif block in NW Morocco with respect to the Nubian plate (Fadil et al., 2006; Koulali et al., 2011). From dynamic modeling of GPS velocities, the SW escape of the Rif has been attributed to horizontal traction applied to the base of the Rif (Pérouse et al., 2010). Our results suggest that traction affects subcrustal material as well, and may originate in the uppermost mantle. A plausible source of traction may be the mantle resistance to slab dragging (Spakman et al., 2018). In fact, absolute plate motions in a model that is constrained to zero net rotation estimate that the lithosphere is moving at rate of ~2.5 cm/year in NW direction (~N40°E; Kreemer et al., 2014) with respect to the underlying mantle, in agreement with the dominant direction of *P* axes.

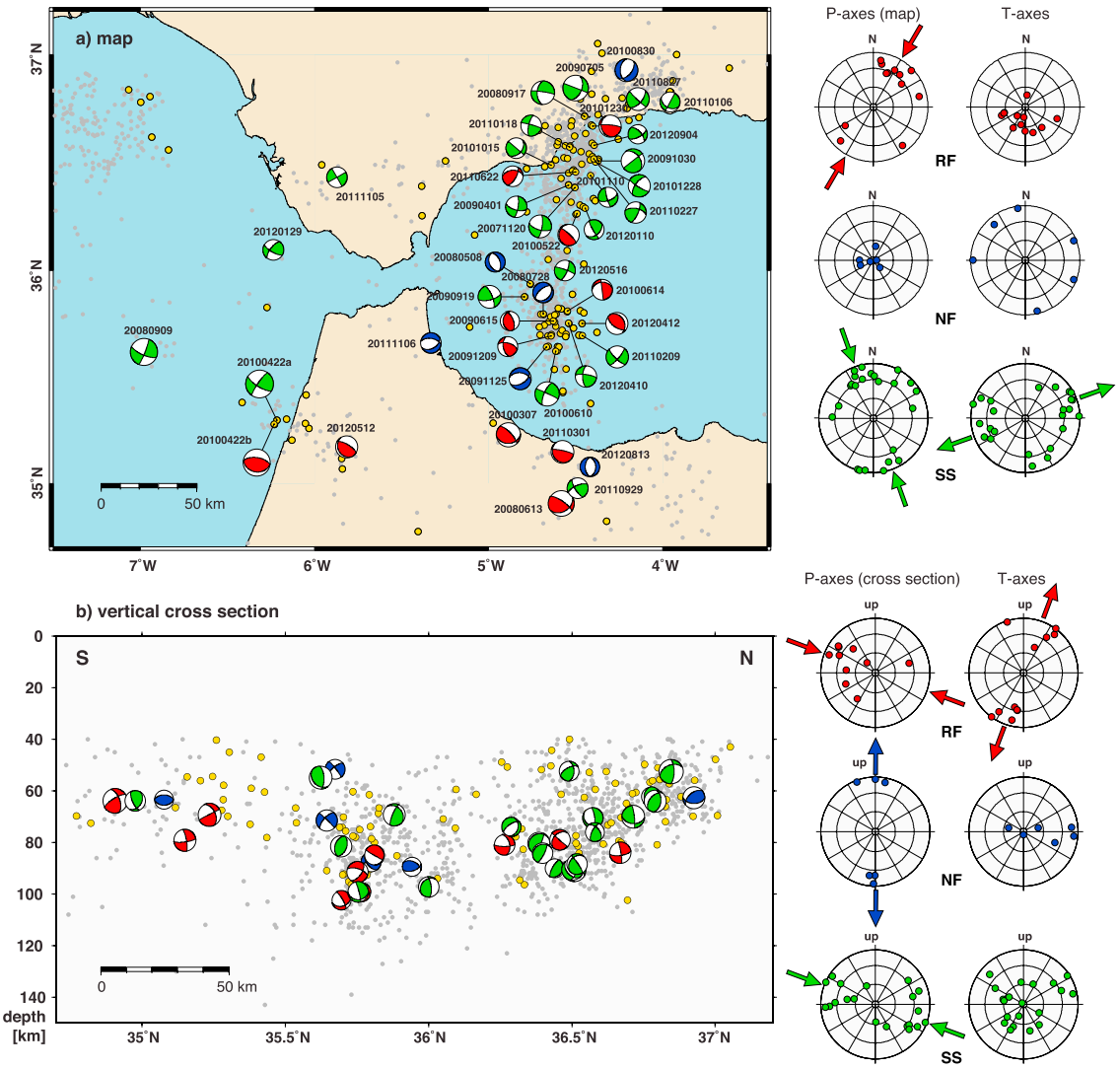

Figure 3. (a) Left: focal mechanisms for reverse (red), normal (blue), and strike-slip faulting earthquakes (green). Intermediate deep seismicity from the Instituto Geográfico Nacional catalogue (gray dots) and relocations in this study (yellow dots) are given for reference. Right: lower hemisphere projection of *P* and *T* axes for the three different faulting styles. Arrows mark dominant directions of principal axes (compare Figures S2 and S3). (b) Left: hypocenters and mechanisms between 4°W and 5°W projected into a vertical section. Right: projections of *P* and *T* axes into vertical section.

The most abundant solutions among our inventory are strike-slip events, representing 24 out of 42 mechanisms. This is highly unusual for intermediate depth seismicity, generally characterized by dip-slip faulting associated to strain aligned with the descending slab. Other intermediate depth strike-slip events that occur beneath Pamir or the Indo-Myanmar Ranges were attributed to horizontal plate motion rather than subduction dynamics (Kufner et al., 2016; Rao & Kumar, 1999). In our study, a number of strike-slip solutions responds to NE-SW oriented *P* axes (Figures 3, S2, and S3), coincident with the direction of reverse faulting as well as absolute plate motion. The greater part of strike-slip mechanisms corresponds to approximately NNW-SSE directed *P* axes. This agrees with the crustal stress field and the kinematics of shallow strike-slip events beneath the Gulf of Cadiz and Alboran Sea (e.g., Stich et al., 2005, 2006). In particular, the right-lateral nodal planes reproduce the orientation and kinematics of mayor WNW-ESE trending faults in the Gulf of Cadiz (Zitellini et al., 2009), which are known to host strike-slip earthquakes at crustal and subcrustal depths down to ~55 km (Bartolomé et al., 2012; Geissler et al., 2010). From the observed similarity of shallow and intermediate deep deformation, we associate the predominant strike-slip faulting solutions in the slab with the right-lateral transcurrent motion between the African and Eurasian plates, which is reproduced

at uppermost mantle level. The right-lateral nodal planes of the predominant strike-slip faulting mechanisms follow the ~N300°E direction of relative plate motion (Kreemer et al., 2014), explaining the observed concentration of *P* axes in NNW-SSE direction.

A smaller number of solutions show normal faulting mechanisms with variable azimuths. In contrast to reverse and strike-slip solutions, the normal faulting mechanisms do not present notable obliqueness, and maximum principal strain is subvertical in all cases (plunge ≥69°). This suggests that they are driven by buoyancy. While the population of normal faulting solutions is possibly too small and heterogeneous to draw firm conclusions, their occurrence may be a consequence of advanced slab tearing at shallow depth (e.g., Heit et al., 2017), putting an end to slab pull from the negative buoyancy contrast between cold, subducting mantle lithosphere and the surrounding asthenosphere. In summary, the abundance of strike-slip faulting as well as the lack of orientation in dip-slip focal mechanisms do not support a scenario of active subduction where intermediate deep seismicity is controlled by downdip stresses transmitted through the viscous slab (Chen et al., 2004; Isacks & Molnar, 1971).

4. Oceanic or Continental?

Intermediate deep seismicity is commonly related to subduction of oceanic lithosphere, although faulting in the upper continental mantle has been reported (Malusà et al., 2017; Prieto et al., 2017). In the Alboran-Gibraltar region, the association of intermediate depth earthquakes with oceanic or continental material is not clear beforehand, and beyond the explanatory potential of current tomographic models. Subduction beneath the Gibraltar Arc appears no longer active, the available oceanic lithosphere of the Alboran slab could have been consumed, and present intermediate deep activity could occur in a continental environment. According to *P* wave receiver functions (Mancilla et al., 2013; Mancilla, Booth-Rea, et al., 2015; Mancilla, Stich, et al., 2015), the Iberian crust is underthrusting the Alboran crust in southern Spain, and earthquakes down to ~60 km at the Spanish coast can be associated with continental lithosphere (Morales et al., 1999; Ruiz-Constán et al., 2011). Although continental lithosphere is not prone to subduct, it still may be carried down to at least 100-km depth according to observations of high-pressure metamorphic rocks (Ernst, 1999). This would cover the full depth range of Alboran intermediate deep seismicity.

The assignment of intermediate seismicity to oceanic lithosphere may be postulated from the possible connection in Mesozoic times between the spreading centers of the Alpine Tethys and the Central Atlantic. Paleogeographic reconstructions suggest the formation of a narrow oceanic corridor between Iberia and Africa in the Jurassic (Frizon de Lamotte et al., 2011; Stampfli & Borel, 2002; Vergés & Fernàndez, 2012). This view is supported by sharp transitions between oceanic and continental domains in the Gulf of Cadiz, suggesting the continuity of Tethys transform faults into this sector (Ramos et al., 2017; Sallarès et al., 2011). This scenario implies the presence of oceanic lithosphere under the Gibraltar Arc, a connection to the autochthonous oceanic crust in the Atlantic, and the oceanic nature of the retreating Alboran slab, at least in its central part (Molina-Aguilera et al., 2019). Having said that, alternative reconstructions suggest that the Tethys margin between Iberia and Africa was formed by a transcurrent fault in continental crust (Rosenbaum et al., 2002; Seton et al., 2012). This model could be consistent with low velocities inferred under the Gibraltar Arc (Monna et al., 2013; Palomeras et al., 2014; Thurner et al., 2014).

Here we reanalyze teleseismic *P* wave conversions beneath the Gibraltar Arc recorded in receiver functions from permanent and temporary broadband stations (Mancilla, Booth-Rea, et al., 2015; Mancilla, Stich, et al., 2015). We attempt to resolve details of the Moho topography from multiple reverberated phases, in particular the *PpPs* and *PsPs* + *PpSs* phases. The reverberations show high sensitivity to Moho topography due to their longer travel path involving multiple legs within the crust. We build common conversion point stacking images through backprojection of the *P* wave receiver functions along their incident ray path taking into account the increase of the width of the Fresnel zone with depth. We stack in the cross-section all receiver function samples with piercing points within 50-km distance from the profile. In these profiles, positive values (primary *P*-to-*S* conversion at the Moho, as well as *PpPs* phases) are shown in red, and negative values (*PsPs* + *PpSs* phases) in blue (Figure 4). We may locate the Moho discontinuity at the base of the initial velocity increase and support the result from analyzing crustal reverberations. The reverberations are not migrated to their correct geometrical position, and experiment vertical stretching by a factor of more than two, which allows resolving Moho topography below 5 km.

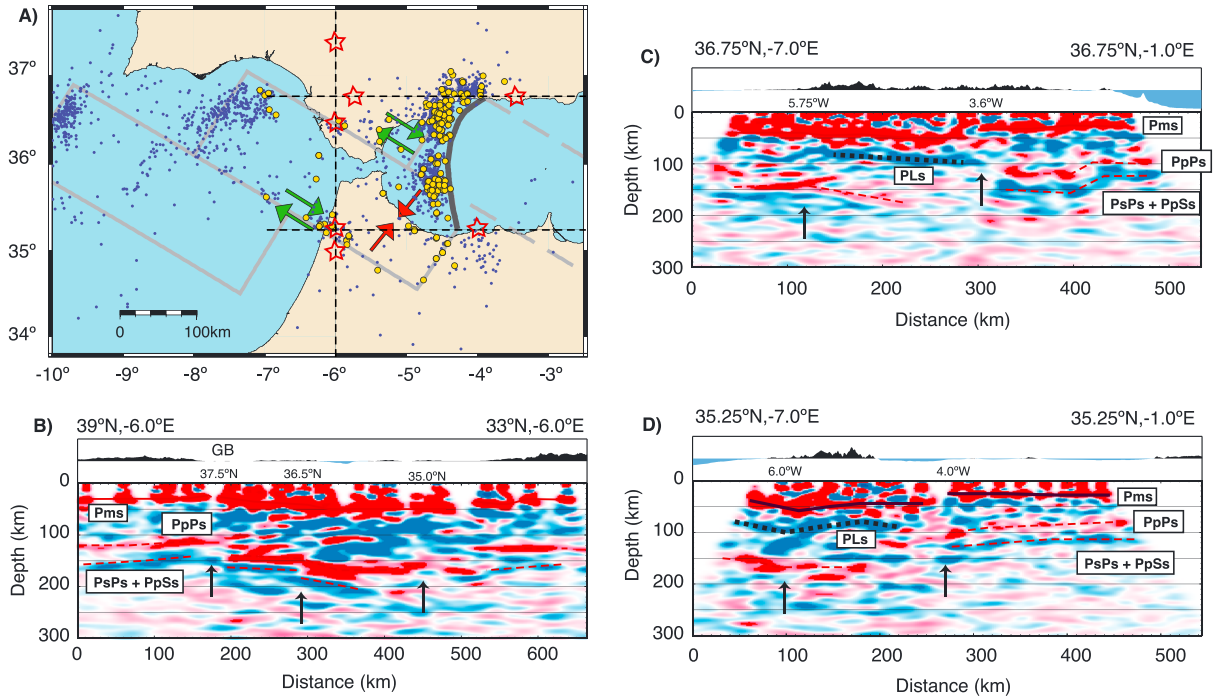

Figure 4. (a) Schematic sketch of the geometry of Tethys oceanic lithosphere beneath the Gibraltar Arc and Gulf of Cadiz, consistent with the distribution of subcrustal earthquakes (yellow: relocated; blue: Instituto Geográfico Nacional catalogue) and migrated receiver function images along profiles in N-S (b) and W-E (c, d) direction (thin lines in a). Red color corresponds to positive amplitudes (velocity increase with depth) and blue to negative amplitudes. Continuous black lines mark the inferred conversion depth of the *Ps* converted phase at the Moho discontinuity (*Pms*, positive amplitudes) and dotted black lines the *Ps* converted phase at the LAB discontinuity (*PLs*, negative amplitudes). Dashed black lines mark the first reverberated phases (*PpPs* and *PsPs + PpSs*) generated at the Moho discontinuity. Stars in (a) and arrows in (b)–(d) mark bends and offsets in Moho topography.

The migrated cross sections (Figure 4) indicate crustal thickness in excess of 40 km under most of the Gibraltar Arc (Mancilla, Booth-Rea, et al., 2015; Mancilla, Stich, et al., 2015). The image of the deepest Moho levels in multiple reverberated phases is delimited by rather abrupt offsets of around 20 km, corresponding to actual Moho depth variations between 5 and 10 km. These values agree with the thickness of regular oceanic crust, providing support for a scenario where the Gibraltar Arc was built, in fact, by the overthrusting of the allochthonous units onto preexisting oceanic lithosphere (Molina-Aguilera et al., 2019; Ramos et al., 2017; Vergés & Fernàndez, 2012). Although teleseismic *P* wave conversions do not sample the central Alboran Sea, available data show a general match between the extension of thickened crust, the occurrence of intermediate depth seismicity, and the expected geometry for a segmented corridor of oceanic lithosphere beneath the Gibraltar Arc (Frizon de Lamotte et al., 2011; Stampfli & Borel, 2002). Coincident Moho offsets and WNW-ESE lineaments of intermediate depth seismicity (Figures 4b and 4d) can be associated with Tethys transform faults inferred from structural images (Ramos et al., 2017; Sallarès et al., 2011). This is in agreement with right-lateral strike-slip deformation inferred from focal mechanisms. Receiver function images support the presence of remnant oceanic crust flooring the Gibraltar Arc, and a former connection between the Alpine Tethys and the central Atlantic spreading centers. The oceanic corridor currently hosts intermediate depth seismicity in its interior and particularly along the limits of the most thickened crust (compare Figures 1 and 4). Other intermediate deep earthquakes occur outside the autochthonous oceanic lithosphere, in particular beneath the Spanish coast where earthquakes can be associated with continental delamination (Mancilla et al., 2013).

5. Conclusions

Dense temporal deployments in the Betic-Rif region help evaluating subcrustal earthquakes and lithospheric structure. Intermediate depth seismicity in a ~200-km-wide band under the Gibraltar Arc has been relocated with maximum depth of ~70 km. This is notably deeper than earthquakes beneath the eastern Atlantic, which occur down to ~55 km, in agreement with the expected limit of brittle faulting in Jurassic

age oceanic lithosphere in situ (Geissler et al., 2010; Stich et al., 2005). Receiver function images give hints for the oceanic nature of the lithosphere beneath the Gibraltar Arc, which hosts part of the upper mantle seismicity. Seismicity beneath the Spanish coast may be attributed to delamination (Mancilla et al., 2013). Beneath the central Alboran Sea, intermediate depth seismicity has larger depth extend from 50 to ~100 km, which may correspond to the bending of oceanic lithosphere into the near-vertical Alboran slab seen in tomographic images. Alboran earthquakes do not depict a Wadati Benioff zone, and the slab may be affected by lithospheric tearing, related to a recognized transfer fault system onshore (Heit et al., 2017; Mancilla et al., 2018).

Forty-two new focal mechanisms in this study lack a clear relation with downdip stresses and suggest that subduction of the Alboran slab has come to a halt or slowed down significantly. The prevalent strike-slip faulting solutions agree with the present-day plate motion between Nubia and Eurasia, as well as with the orientation of the transform faults of the Alpine Tethys (approximately WNW-ESE in present coordinates; Frizon de Lamotte et al., 2011). Mechanisms with NE-SW directed compression axes are the second major trend, in-line with absolute plate motion of the Alboran region, which is substantially different from relative plate motion in terms of rate (~2.5 cm/year) and direction (~N40°E; Kreemer et al., 2014). This direction also characterizes compression in NW Morocco, providing support for a deep origin of the emplacement of the Rif mountains in direction perpendicular to current plate motion. Motion of the Rif has been attributed to slab rollback (Pérouse et al., 2010), although upper mantle anisotropy (Diaz et al., 2010) indicates mantle flow perpendicular to the escape of the Rif. SW directed drag on the mantle lithosphere (Spakman et al., 2018) may provide a more simple explanation for deformation of the Alboran slab and NW Morocco.

Acknowledgments
We are grateful to all individuals and institutions involved in the IberArray and Picasso deployments, and the maintenance of permanent networks. We appreciate the useful comments by Andreas Fichtner and an anonymous reviewer. Velocities of tectonic plates were retrieved from the Unavco Plate motion calculator (www.unavco.org). We used free software Seisan (Havskov & Ottemoller, 1999) and GMT (Wessel & Smith, 1998). We received financial support through Mineco/Feder Project CGL2015-67130-C2-2-R and Junta de Andalucía research group RNM 104.

References

Bartolomé, R., Gràcia, E., Stich, D., Martínez–Loriente, S., Klaeschen, D., Mancilla, F., et al. (2012). Evidence for active strike-slip faulting along the Eurasia-Africa convergence zone: Implications for seismic hazard in the southwest Iberian margin. *Geology*, *40*(6), 495–498. https://doi.org/10.1130/G33107.1

Bezada, M. J., Hymphreys, E. D., Toomey, D. R., Harnafi, M., Dávila, J. M., & Gallart, J. (2013). Evidence for slab rollback in westernmost Mediterranean from improved upper mantle imaging. *Earth and Planetary Science Letters*, *368*, 51–60. https://doi.org/10.1016/j.epsl.2013.02.024

Bonnin, M., Nolet, G., Villaseñor, A., Gallart, J., & Thomas, C. (2014). Multiple-frequency tomography of the upper mantle beneath the African/Iberian collision zone. *Geophysical Journal International*, *198*(3), 1458–1473. https://doi.org/10.1093/gji/ggu214

Buforn, E., Bezzeghoud, M., Udías, A., & Pro, C. (2004). Seismic sources on the Iberia-African plate boundary and their tectonic implications. *Pure and Applied Geophysics*, *161*(3), 623–646. https://doi.org/10.1007/s00024-003-2466-1

Buforn, E., & Coca, P. (2002). Seismic moment tensor for intermediate depth earthquakes at regional distances in Southern Spain. *Tectonophysics*, *356*(1-3), 49–63. https://doi.org/10.1016/S0040-1951(02)00376-1

Buforn, E., Pro, C., Cesca, S., Udías, A., & del Fresno, C. (2011). The 2010 Granada, Spain, deep earthquake. *Bulletin of the Seismological Society of America*, *101*(5), 2418–2430. https://doi.org/10.1785/0120110022

Calvert, A., Sandvol, E., Seber, D., Barazangi, M., Roecker, S., Mourabit, T., et al. (2000). Geodynamic evolution of the lithosphere and upper mantle beneath the Alboran region of the western Mediterranean: Constraints from travel time tomography. *Journal of Geophysical Research*, *105*(B5), 10,871–10,898. https://doi.org/10.1029/2000JB900024

Chen, P.-F., Bina, C. R., & Okal, E. A. (2004). A global survey of stress orientations in subducting slabs as revealed by intermediate depth earthquakes. *Geophysical Journal International*, *159*(2), 721–733. https://doi.org/10.1111/j.1365-246X.2004.02450.x

Christova, C., & Scholz, C. H. (2003). Stresses in the Vanuatu subducting slab: A test of two hypotheses. *Geophysical Research Letters*, *30*(15), 1790. https://doi.org/10.1029/2003GL017701

Comas, M. C., García-Dueñas, V., & Jurado, M. J. (1992). Neogene tectonic evolution of the Alboran Sea from MCS data. *Geo-Marine Letters*, *12*(2–3), 157–164. https://doi.org/10.1007/BF02084927

Diaz, J., Gallart, J., Villaseñor, A., Mancilla, F., Pazos, A., Córdoba, D., et al. (2010). Mantle dynamics beneath the Gibraltar Arc (western Mediterranean) from shear-wave splitting measurements on a dense seismic array. *Geophysical Research Letters*, *37*, L18304. https://doi.org/10.1029/2010GL044201

Ernst, W. G. (1999). Metamorphism, partial preservation, and exhumation of ultrahigh-pressure belts. *Island Arc*, *8*(2), 125–153. https://doi.org/10.1046/j.1440-1738.1999.00227.x

Faccenna, C., Piromallo, C., Crespo-Blanc, A., Jolivet, L., & Rossetti, F. (2004). Lateral slab deformation and the origin of the western Mediterranean arcs. *Tectonics*, *23*, TC1012. https://doi.org/10.1029/2002TC001488

Fadil, A., Vernant, P., McClusky, S., Reilinger, R., Gomez, F., Sari, D. B., et al. (2006). Active tectonics of the western Mediterranean: Geodetic evidence for roll back of a delaminated subcontinental lithospheric slab beneath the Rif Mountains, Morocco. *Geology*, *34*(7), 529–532. https://doi.org/10.1130/G22291.1

Fichtner, A., & Villaseñor, A. (2015). Crust and upper mantle of the western Mediterranean—Constraints from full-waveform inversion. *Earth and Planetary Science Letters*, *428*, 52–62. https://doi.org/10.1016/j.epsl.2015.07.038

Frizon de Lamotte, D., Raulin, C., Mouchot, N., Wrobel-Daveau, J. C., Blanpied, C., & Ringenbach, J. C. (2011). The southernmost margin of the Tethys realm during the Mesozoic and Cenozoic: Initial geometry and timing of the inversion processes. *Tectonics*, *30*, TC3002. https://doi.org/10.1029/2010TC002691

Gallart, J., Carbonell, R., & Diaz, J. (2012). TOPOIBERIA and its array infrastructure IBERARRAY. EPOS newsletter 4, 2. Retrieved from www.epos-eu.org

Geissler, W. H., Matias, L., Stich, D., Carrilho, F., Jokat, W., Monna, S., et al. (2010). Focal mechanisms for sub-crustal earthquakes in the Gulf of Cadiz from a dense OBS deployment. *Geophysical Research Letters*, *37*, L18309. https://doi.org/10.1029/2010GL044289

Gutscher, M.-A., Dominguez, S., Westbrook, G. K., Le Roy, P., Rosas, F., Duarte, J. C., et al. (2012). The Gibraltar subduction: A decade of new geophysical data. *Tectonophysics*, *574-575*, 72–91. https://doi.org/10.1016/j.tecto.2012.08.038

Gutscher, M.-A., Malod, J., Rehault, J.-P., Contrucci, I., Klingelhoefer, F., Mendes-Victor, L., & Spakman, W. (2002). Evidence for active subduction beneath Gibraltar. *Geology*, *30*(12), 1071–1074. https://doi.org/10.1130/0091-7613(2002)030<1071:EFASBG>2.0.CO;2

Havskov, J., & Ottemoller, L. (1999). SeisAn earthquake analysis software. *Seismological Research Letters*, *70*(5), 532–534. https://doi.org/10.1785/gssrl.70.5.532

Heit, B., Mancilla, F., Yuan, X., Morales, J., Stich, D., Martín, R., & Molina-Aguilera, A. (2017). Tearing of the mantle lithosphere along the intermediate-depth seismicity zone beneath the Gibraltar Arc: The onset of lithospheric delamination. *Geophysical Research Letters*, *44*, 4027–4035. https://doi.org/10.1002/2017GL073358

Isacks, B., & Molnar, P. (1971). Distribution of stresses in the descending lithosphere from a global survey of focal-mechanism solutions of mantle earthquakes. *Reviews of Geophysics*, *9*(1), 103–174. https://doi.org/10.1029/RG009i001p00103

Kagan, Y. (2007). Simplified algorithms for calculating double-couple rotation. *Geophysical Journal International*, *171*(1), 411–418. https://doi.org/10.1111/j.1365-246X.2007.03538.x

Koulali, A., Ouazar, D., Tahayt, A., King, R. W., Vernant, P., Reilinger, R. E., et al. (2011). New GPS constraints on active deformation along the Africa–Iberia plate boundary. *Earth and Planetary Science Letters*, *308*(1-2), 211–217. https://doi.org/10.1016/j.epsl.2011.05.048

Kreemer, C., Blewitt, G., & Klein, E. C. (2014). A geodetic plate motion and Global Strain Rate Model. *Geochemistry, Geophysics, Geosystems*, *15*, 3849–3889. https://doi.org/10.1002/2014GC005407

Kufner, S.-K., Schurr, B., Sippl, C., Yuan, X., Ratschbacher, L., Akbar, A. ./. M., et al. (2016). Deep India meets deep Asia: Lithospheric indentation, delamination and break-off under Pamir and Hindu Kush (Central Asia). *Earth and Planetary Science Letters*, *435*, 171–184. https://doi.org/10.1016/j.epsl.2015.11.046

Levander, A., Humphreys, G., & Ryan, P. (2009). Program to investigate convective Alboran Sea system overturn. International Federation of Digital Seismograph Networks. Other/Seismic Network. https://doi.org/10.7914/SN/XB_2009

Lienert, B. R. E., & Havskov, J. (1995). A computer program for locating earthquakes both locally and globally. *Seismological Research Letters*, *66*(5), 26–36. https://doi.org/10.1785/gssrl.66.5.26

Lonergan, L., & White, N. (1997). Origin of the Betic-Rif mountain belt. *Tectonics*, *16*(3), 504–522. https://doi.org/10.1029/96TC03937

Malusà, M. G., Zhao, L., Eva, E., Solarino, S., Paul, A., Guillot, S., et al. (2017). Earthquakes in the western Alpine mantle wedge. *Gondwana Research*, *44*, 89–95. https://doi.org/10.1016/j.gr.2016.11.012

Mancilla, F., Booth-Rea, G., Stich, D., Pérez-Peña, J. V., Morales, J., Azañón, J. M., et al. (2015). Slab rupture and delamination under the Betics and Rif constrained from receiver functions. *Tectonophysics*, *663*, 225–237. https://doi.org/10.1016/j.tecto.2015.06.028

Mancilla, F., & Diaz, J. (2015). High resolution Moho topography map beneath Iberia and Northern Morocco from receiver function analysis. *Tectonophysics*, *663*, 203–211. https://doi.org/10.1016/j.tecto.2015.06.017

Mancilla, F., Heit, B., Morales, J., Yuan, X., Stich, D., Molina-Aguilera, A., et al. (2018). A STEP fault in Central Betics, associated with lateral lithospheric tearing at the northern edge of the Gibraltar arc subduction system. *Earth and Planetary Science Letters*, *486*, 32–40. https://doi.org/10.1016/j.epsl.2018.01.008

Mancilla, F., Stich, D., Berrocoso, M., Martin, R., Morales, J., Fernández-Ros, A., et al. (2013). Delamination in the Betic Range: Deep structure, seismicity, and GPS motion. *Geology*, *41*(3), 307–310. https://doi.org/10.1130/G33733.1

Mancilla, F., Stich, D., Morales, J., Martín, R., Diaz, J., Pazos, A., et al. (2015). Crustal thickness and images of the lithospheric discontinuities in the Gibraltar arc and surrounding areas. *Geophysical Journal International*, *203*, 1804–1820. https://doi.org/10.1093/gji/ggv390

Martín, R., Stich, D., Morales, J., & Mancilla, F. (2015). Moment tensor solutions for the Iberian-Maghreb region during the Iberarray deployment. *Tectonophysics*, *663*, 261–274. https://doi.org/10.1016/j.tecto.2015.08.012

Medina F. (2008). Catalogue of focal mechanisms of the Moroccan earthquakes for the period 1959-2007. *Doc. Inst. Sci., Rabat, 23*, 56 p.

Molina-Aguilera, A., Mancilla, F., Morales, J., Stich, D., Yuan, X., & Heit, B. (2019). Connection between the Jurassic oceanic lithosphere of the Gulf of Cádiz and the Alboran slab imaged by Sp receiver functions. *Geology*, *47*(3), 227–230. https://doi.org/10.1130/G45654.1

Monna, S., Cimini, G. B., Montuori, C., Matias, L., Geissler, W. H., & Favali, P. (2013). New insights from seismic tomography on the complex geodynamic evolution of two adjacent domains: Gulf of Cadiz and Alboran Sea. *Journal of Geophysical Research: Solid Earth*, *118*, 1587–1601. https://doi.org/10.1029/2012JB009607

Morales, J., Serrano, I., Jabaloy, A., Galindo-Zaldivar, J., Zhao, D., Torcal, F., et al. (1999). Active continental subduction beneath the Betic cordillera and Alboran Sea. *Geology*, *27*(8), 735–738. https://doi.org/10.1130/0091-7613(1999)027<0735:ACSBTB>2.3.CO;2

Myhill, R., & Warren, L. M. (2012). Fault plane orientations of deep earthquakes in the Izu-Bonin-Marianas subduction zone. *Journal of Geophysical Research*, *117*, B06307. https://doi.org/10.1029/2011JB009047

Palomeras, I., Thurner, S., Levander, A., Liu, K., Villasenor, A., Carbonell, R., & Harnafi, M. (2014). Finite-frequency Rayleigh wave tomography of the western Mediterranean: Mapping its lithospheric structure. *Geochemistry, Geophysics, Geosystems*, *15*, 140–160. https://doi.org/10.1002/2013GC004861

Palomeras, I., Villaseñor, A., Thurner, S., Levander, A., Gallart, J., & Harnafi, M. (2017). Lithospheric structure of Iberia and Morocco using finite-frequency Rayleigh wave tomography from earthquakes and seismic ambient noise. *Geochemistry, Geophysics, Geosystems*, *18*, 1824–1840. https://doi.org/10.1002/2016GC006657

Pérouse, E, Vernant, P., Chery, J., Reilinger, R., &. McClusky, S. (2010). Active surface deformation and sub-lithospheric processes in the western Mediterranean constrained by numerical models. *Geology 38*(9), 823–826.https://doi.org/10.1130/G30963.1

Piromallo, C., & Morelli, A. (2003). P wave tomography of the mantle under the Alpine-Mediterranean area. *Journal of Geophysical Research*, *108*(B2), 2065. https://doi.org/10.1029/2002JB001757

Platt, J. P., & Vissers, R. L. M. (1989). Extensional collapse of thickened continental lithosphere; a working hypothesis for the Alboran Sea and Gibraltar Arc. *Geology*, *17*(6), 540–543. https://doi.org/10.1130/0091-7613(1989)017<0540:ECOTCL>2.3.CO;2

Prieto, G. A., Froment, B., Yu, C., Poli, P., & Abercrombie, R. (2017). Earthquake rupture below the brittle-ductile transition in continental lithospheric mantle. *Science Advances*, *3*(3), e1602642. https://doi.org/10.1126/sciadv.1602642

Ramos, A., Fernández, O., Torne, M., Sánchez de la Muela, A., Muñoz, J. A., Terrinha, P., et al. (2017). Crustal structure of the SW Iberian passive margin: The westernmost remnant of the Ligurian Tethys? *Tectonophysics*, *705*, 42–62. https://doi.org/10.1016/j.tecto.2017.03.012

Rao, N. P., & Kumar, M. R. (1999). Evidences for cessation of Indian plate subduction in the Burmese arc region. *Geophysical Research Letters*, *26*(20), 3149–3152. https://doi.org/10.1029/1999GL005396

Rosenbaum, G., Lister, G. S., & Duboz, C. (2002). Relative motions of Africa, Iberia and Europe during Alpine orogeny. *Tectonophysics*, *359*(1-2), 117–129. https://doi.org/10.1016/S0040-1951(02)00442-0

Rueda, J. (1995). Análisis y procesamiento de datos en la Red Sísmica Nacional. En: *Redes Sísmicas Regionales*, Monografías I.G.N., Madrid, 11, 87–111.

Ruiz-Constán, A., Galindo-Zaldívar, J., Pedrera, A., Célérier, B., & Marín-Lechado, C. (2011). Stress distribution at the transition from subduction to continental collision (northwestern and central Betic Cordillera). *Geochemistry, Geophysics, Geosystems*, *12*, Q12002. https://doi.org/10.1029/2011GC003824

Sallarès, V., Gailler, A., Gutscher, M. A., Graindorge, D., Bartolomé, R., Gràcia, E., et al. (2011). Seismic evidence for the presence of Jurassic oceanic crust in the central Gulf of Cadiz (SW Iberian margin). *Earth and Planetary Science Letters*, *311*(1-2), 112–123. https://doi.org/10.1016/j.epsl.2011.09.003

Seber, D., Barazangi, M., Ibenbrahim, A., & Demnati, A. (1996). Geophysical evidence for lithospheric delamination beneath the Alboran Sea and Rif-Betic mountains. *Nature*, *379*(6568), 785–790. https://doi.org/10.1038/379785a0

Seton, M., Müller, R. D., Zahirovic, S., Gaina, C., Torsvik, T., Shephard, G., et al. (2012). Global continental and ocean basin reconstructions since 200 Ma. *Earth-Science Reviews*, *113*(3-4), 212–270. https://doi.org/10.1016/j.earscirev.2012.03.002

Snoke, J. A., Munsey, J. W., Teague, A. G., & Bollinger, G. A. (1984). A program for focal mechanism determination by combined use of polarity and SV-P amplitude ratio data. *Earthquake Notes*, *5*(2), 165–171. https://doi.org/10.1007/BF02910422

Spakman, W, Chertova, M., Berg A., & Hinsbergen, D. (2018). Puzzling features of western Mediterranean tectonics explained by slab dragging. *Nature Geoscience 11*(3), 374. https://doi.org/10.1038/s41561-018-0066-z

Spakman, W., & Wortel, R. (2004). A tomographic view on Western Mediterranean geodynamics. In W. Cavazza, et al. (Eds.), *The TRANSMED Atlas: The Mediterranean Region From Crust to Mantle* (pp. 31–52). Berlin: Springer. https://doi.org/10.1007/978-3-642-18919-7_2

Stampfli, G. M., & Borel, G. D. (2002). A plate tectonic model for the Paleozoic and Mesozoic constrained by dynamic plate boundaries and restored synthetic oceanic isochrons. *Earth and Planetary Science Letters*, *196*(1-2), 17–33. https://doi.org/10.1016/S0012-821X(01)00588-X

Stich, D., Ammon, C. J., & Morales, J. (2003). Moment tensor solutions for small and moderate earthquakes in the Ibero-Maghreb region. *Journal of Geophysical Research*, *108*(B3), 2148. https://doi.org/10.1029/2002JB002057

Stich, D., Mancilla, F., & Morales, J. (2005). Crust-mantle coupling in the Gulf of Cadiz (SW-Iberia). *Geophysical Research Letters*, *32*, L13306. https://doi.org/10.1029/2005GL023098

Stich, D., Serpelloni, E., Mancilla, F., & Morales, J. (2006). Kinematics of the Iberia-Maghreb plate contact from seismic moment tensors and GPS observations. *Tectonophysics*, *426*(3-4), 295–317. https://doi.org/10.1016/j.tecto.2006.08.004

Thurner, S., Palomeras, I., Levander, A., Carbonell, R., & Lee, C.-T. (2014). Ongoing lithospheric removal in the western Mediterranean: Evidence from Ps receiver functions and thermobarometry of Neogene basalts (PICASSO project). *Geochemistry, Geophysics, Geosystems*, *15*, 1113–1127. https://doi.org/10.1002/2013GC005124

Vergés, J., & Fernàndez, M. (2012). Tethys–Atlantic interaction along the Iberia–Africa plate boundary: The Betic–Rif orogenic system. *Tectonophysics*, *579*, 144–172. https://doi.org/10.1016/j.tecto.2012.08.032

Wessel, P., & Smith, W. H. F. (1998). New, improved version of the generic mapping tools released. *EOS Transactions American Geophysical Union*, *79*(47), 579. https://doi.org/10.1029/98EO00426

Zitellini, N., Gràcia, E., Matias, L., Terrinha, P., Abreu, M. A., DeAlteriis, G., et al. (2009). The quest for the Africa-Eurasia plate boundary west of the strait of Gibraltar. *Earth and Planetary Science Letters*, *280*(1-4), 13–50. https://doi.org/10.1016/j.epsl.2008.12.005